9-7-2011

Spatial Correlation of Interseismic Coupling and Coseismic Rupture Extent of the 2011 MW=9.0 Tohoku-Oki Earthquake

John P. Loveless
Harvard University, jloveles@smith.edu

Brendan J. Meade
Harvard University

Spatial correlation of interseismic coupling and coseismic rupture extent of the 2011 M_W = 9.0 Tohoku-oki earthquake

John P. Loveless[1,2] and Brendan J. Meade[1]

Received 16 June 2011; revised 1 August 2011; accepted 2 August 2011; published 7 September 2011.

[1] Imaging the extent to which the rupture areas of great earthquakes coincide with regions of pre-seismic interplate coupling is central to understanding patterns of strain accumulation and release through the earthquake cycle. Both geodetic and seismic estimates of the coseismic rupture extent for the March 11, 2011 M_W = 8.9–9.0 earthquake Tohoku-oki earthquake may be spatially correlated (0.26 ± 0.05 to 0.82 ± 0.05) with a region estimated to be partially to fully coupled in the interseismic period preceding the earthquake, though there is substantial variation in the estimated distribution and magnitude of coseismic slip. The ~400 km-long region estimated to have slipped ≥4 m corresponds to an area of the subduction zone interface that was coupled at ≥30% of long-term plate convergence rate, with peak slip near a region coupled ≥80%. The northern termination of rupture is collocated with a region of relatively low (<20%) interseismic coupling near the epicenter of the 1994 M_W = 7.6 Sanriku-oki earthquake, and near a region of potential long-term low coupling or ongoing slow slip. Slip on the subduction interface beneath the coastline (40–50 km depth) is best constrained by the land-based GPS data and least constrained on the shallowest portion of the plate interface due to the ~230 km distance between geodetic observations and the Japan trench. **Citation:** Loveless, J. P., and B. J. Meade (2011), Spatial correlation of interseismic coupling and coseismic rupture extent of the 2011 M_W = 9.0 Tohoku-oki earthquake, *Geophys. Res. Lett.*, *38*, L17306, doi:10.1029/2011GL048561.

1. Introduction

[2] Recent studies have investigated the extent to which geodetically imaged pre-seismic interplate coupling defines the area of coseismic moment release during subsequent great earthquakes. *Konca et al.* [2008] found that two earthquakes on the Sumatra subduction zone in 2007 (M_W = 8.4 and M_W = 7.9) ruptured individual asperities contained within the inferred rupture area of the 1833 M_W = 9.0 event, leaving much of that event's source area still locked. *Moreno et al.* [2010] found that the 2010 M_W = 8.8 Maule, Chile earthquake occurred within a region of the Nazca-South American subduction zone that was geodetically estimated to have been pre-seismically locked, and that the rupture limits may have been defined by the pre-existing stress state shaped by previous earthquakes. These apparent geometric controls on earthquake size have been hypothesized to result from spatial variations in frictional properties [*Kaneko et al.*, 2010] or macroscopic geometric segmentation such as coastline/slab morphology and bathymetric relief on the down-going plate [e.g., *Aki*, 1979; *Cloos*, 1992; *Kelleher and McCann*, 1976].

[3] Geophysical observations of the 2011 Tohoku-oki earthquake off the east coast of Japan have provided much new data to assess the relationship between the spatial distribution of coseismic slip and interseismic coupling. Prior to the occurrence of the Tohoku-oki earthquake, subduction zone coupling distributions were developed based on earthquake cycle models constrained by interseismic GPS data acquired during the seismically quiescent period from 1996–2002. While these models may be divided into those that assume measured deformation is the result of subduction zone earthquake cycle processes exclusively [*Hashimoto et al.*, 2009; *Nishimura et al.*, 2004; *Suwa et al.*, 2006] and those that also incorporate the effects of upper plate faults [*Loveless and Meade*, 2010], coupling distributions from both classes of models are similar at wavelengths of 100–150 km, consistent with the checkerboard resolution tests of *Loveless and Meade* [2010]. Along the Japan-west Kuril subduction interface, interseismic coupling is at a maximum (≥80% of relative plate convergence rate) near the Tokachi-oki (~42°N) and Miyagi-oki (~38°N) regions, and decreases toward a local minimum of 20% near the northeastward bend in the subduction zone strike between Honshu and Hokkaido (Figure 1a).

[4] Large earthquakes over the last decade have ruptured the most strongly coupled patches. The 2003 M_W = 8.0–8.2 Tokachi-oki earthquake occurred on the northern coupled patch, rupturing the same region as inferred for the 1952 M_W = 8.2 Tokachi-oki event [e.g., *Miura et al.*, 2004]. To the south, 3 M_W = 7.0–7.2 earthquakes occurred between 2003 and 2005 offshore Sendai within the most strongly coupled area at 38°N (Figure 1a). The Tohoku-oki earthquake ruptured an area far larger than that estimated to be strongly (≥80%) coupled, slipping >2 m from ~36–40°N latitude and bound at its northern extent by the weakly (≤20%) coupled region near Sanriku-oki (Figure 1a).

2. Tohoku-oki Coseismic Slip Distributions and Pre-Seismic Coupling

[5] Slip distributions for the Tohoku-oki earthquake have been developed based on both seismic and geodetic data and can be compared to the distribution of pre-seismic coupling to assess the spatial relationship between coseismic and interseismic behavior. Before comparing others' models of coseismic slip to interseismic coupling, we develop a geodetically constrained slip distribution on the same three-dimensional fault geometry used previously to estimate inter-

[1]Department of Earth and Planetary Sciences, Harvard University, Cambridge, Massachusetts, USA.
[2]Now at Department of Geosciences, Smith College, Northampton, Massachusetts, USA.

0094-8276/11/2011GL048561

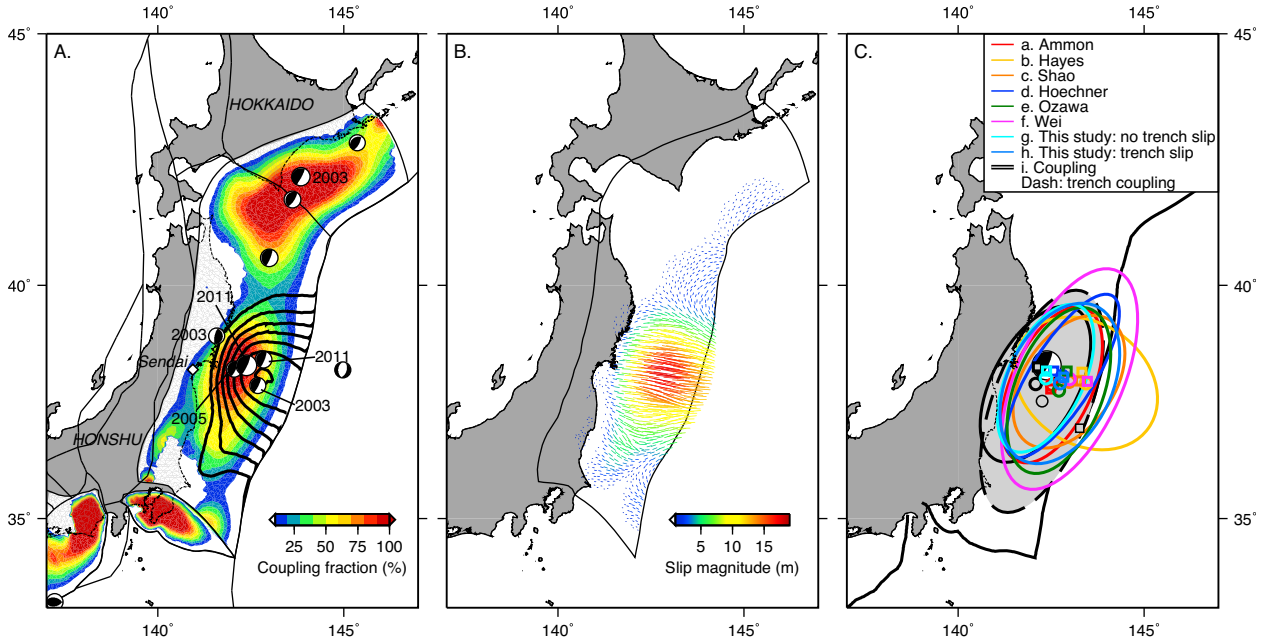

Figure 1. (a) Pre-seismic coupling and seismicity, and coseismic slip of the March 11, 2011 Tohoku-oki earthquake. Coupling, expressed as the fraction of long-term slip represented by coseismic slip deficit ("backslip"), is based on a block model of nominally interseismic horizontal GPS velocities from the GEONET network, 1996–2000 [*Loveless and Meade*, 2010]. Focal mechanisms show earthquakes from the Global CMT catalog with $M_W \geq 7.0$ and depth shallower than 100 km from 1994 up to and including the Tohoku-oki mainshock; year labeled for events mentioned in the text. Coseismic slip, shown as 2.5-m contours, is based on an inversion of GEONET coseismic horizontal displacements from JPL/Caltech [*Simons et al.*, 2011]. The maximum slip is 18 m and the moment magnitude is 8.9. (b) Arrows showing estimated slip vectors, colored by slip magnitude. (c) Comparison of estimates of coseismic slip and pre-seismic coupling (gray ovals; dashed oval is for alternate model in which coupling is permitted at trench). For each distribution, the best-fitting (in a least-squares, algebraic distance sense [*Gander et al.*, 1994]) ellipse through the latitude-longitude pairs of the 4 m slip or 30% coupling contours was estimated. Circles mark ellipse centers and squares mark maximum magnitude. a. *Ammon et al.* [2011], b. Hayes (http://earthquake.usgs.gov/earthquakes/eqinthenews/2011/usc0001xgp/finite_fault.php), c. Shao et al. (http://www.geol.ucsb.edu/faculty/ji/big_earthquakes/2011/03/0311_v3/Honshu.html), d. *Hoechner et al.* [2011], e. *Ozawa et al.* [2011], f. S. Wei et al. (http://tectonics.caltech.edu/slip_history/2011_taiheiyo-oki/index.html), g. this study, with no slip permitted at trench, h. this study, with trench slip permitted.

seismic coupling [*Loveless and Meade*, 2010]. We invert coseismic horizontal GPS displacements at 1216 GEONET stations [*Simons et al.*, 2011] for the distribution of strike- and dip-slip on triangulated tessellation of the Japan Trench megathrust geometry [*Furuse and Kono* [2003] in a homogeneous elastic half-space [*Meade*, 2007]. The inversion is regularized by minimizing the gradient of slip, utilizing the same smoothing coefficient for both strike- and dip-slip components of slip. A reference inversion slip distribution, where the smoothing parameter is chosen such that normal sense slip is less than 10% of the maximum thrust sense slip (rake is not constrained), reaches a maximum of 18 m (82 km from the trench) and yields a moment of $M_0 = 2.59 \times 10^{22}$ Nm ($M_W = 8.88$) (assuming a shear modulus of $G = 30$ GPa; $M_0 = 3.45 \times 10^{22}$ Nm, $M_W = 8.96$ assuming $G = 40$ GPa), with a total area slipping ≥2 m of 8.5×10^4 km^2 (Figure 1a) The moment magnitude is weakly sensitive to the choice of smoothing coefficient; selecting a coefficient 2.25 orders of magnitude smaller than that of our reference inversion results in a moment magnitude of $M_W = 9.00$ (assuming $G = 30$ GPa) and shows a greater magnitude of normal sense slip than thrust.

[6] The maximum magnitude of estimated coseismic slip, 18 m, is similar to some geodetic estimates (21 m, Pollitz (USGS); 23.2 m, Yuuzi and Nishimura (Tsukuba University)) but substantially different from other inversions of seismic and/or geodetic data (36 m, *Hoechner et al.* [2011] (Figure 2d); 40 m, *Ammon et al.* [2011] (Figure 2a); 60 m, *Simons et al.* [2011]; 10 m, Ito et al. (Nagoya University); 28 m, *Ozawa et al.* [2011] (Figure 2e); 33 m, Hayes (USGS) (Figure 2b); ~30 m, Wang (GFZ Potsdam); ~30 m, Wei et al. (Caltech) (Figure 2f); 40 m, Romano et al. (INGV Rome); 60 m, Shao et al. (UCSB) (Figure 2c). All slip estimates from unpublished sources are from http://supersites.earthobservations.org/sendai.php). To simply compare these disparate estimates of coseismic slip with pre-seismic coupling, we reduce each distribution to a single ellipse that best-fits a minimum threshold magnitude of each quantity. We define the ellipses as the algebraic best fit [*Gander et al.*, 1994] to the latitude-longitude pairs of the 4 m coseismic slip contours or the 30% coupling contours (Figure 1c). The magnitude of the semi-major axes highlights the similarity in the latitudinal extent of rupture, both among the different coseismic slip estimates and with the 30% interseismic coupling ellipse, and the clustering of the ellipse centers (circles of Figure 1c). However, despite the availability of densely spaced geodetic and seismic data recording coseismic motion, the estimated maximum slip varies by a factor of >3 in magnitude (18–60 m) and a factor of >2 in depth (11.6–23.9 km; corresponding

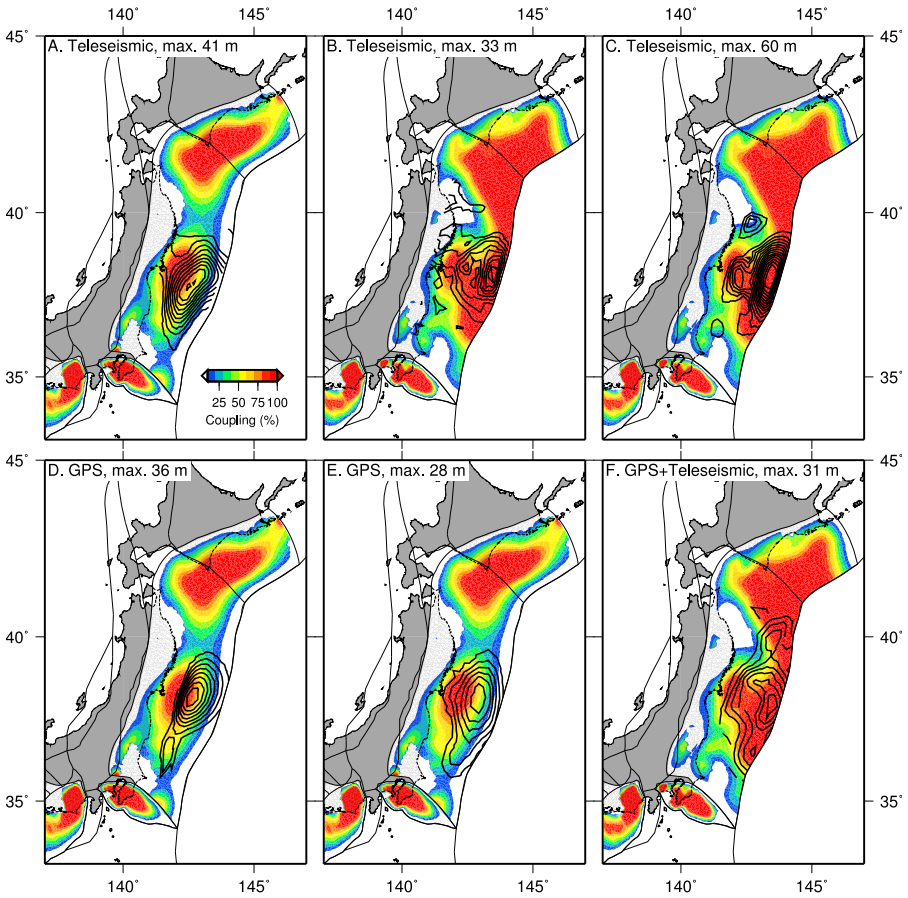

Figure 2. Coseismic slip distributions, shown with 4-m slip contours, from references a–f in Figure 1c, overlain on the reference coupling distribution [*Loveless and Meade*, 2010] or revised coupling distribution, estimated assuming that interseismic strain can accumulate near the trench: whichever is statistically better correlated (Table 1; Figures S1–S6).

range of longitude is 143.5–142.4°E; squares of Figure 1c), reflecting differences in the type of data used, geometric parameterization, rheological assumptions, and/or inversion method (Table 1). Assuming steady interseismic slip deficit of ~85 mm/yr [e.g., *DeMets et al.*, 2010] between earthquakes of this size, the factor of 3 variation in maximum slip requires strain accumulation for 212–706 years, a range substantially less than the time since the 869 AD Jogan earthquake, considered the penultimate great earthquake in the region [*Ozawa et al.*, 2011].

[7] Geodetic data collected prior to the earthquake has been used to estimate the distribution of interseismic coupling on the subduction zone interface that can be compared with coseismic rupture extent. The coupling distribution of *Loveless and Meade* [2010] (Figure 1a; only positive coupling is shown to simplify comparison with coseismic slip) was estimated assuming no interseismic strain accumulation on the up-dip and down-dip edges of the modeled subduction zone interfaces, as the behavior on these elements is less well resolved than is coupling at intermediate depths

Table 1. Coseismic Slip Model Parameters

Model	Constraining Data[a]	Strike[b]/Dip	Coupling Correlation[c]	
			No Trench Coupling	Trench Coupling
a) Ammon et al.	P, R1 RSTF, hrGPS	202°/12°	0.54 ± 0.06	0.54 ± 0.06
b) Hayes	P, SH, surface	195°/10°	0.43 ± 0.10	0.51 ± 0.09
c) Shao et al.	P, SH, surface	198°/10°	0.26 ± 0.13	0.46 ± 0.11
d) Hoechner et al.	GPS (E, N, U)	variable/7–44°	0.82 ± 0.05	0.41 ± 0.12
e) Ozawa et al.	GPS (E, N, U)	variable/0–45°	0.80 ± 0.04	0.37 ± 0.10
f) Wei et al.	P, SH, GPS	193°/14°	0.32 ± 0.10	0.56 ± 0.08
g) This study (no trench slip)	GPS (E, N)	variable/6–47°	0.83 ± 0.02	0.42 ± 0.04
h) This study (trench slip)	GPS (E, N)	variable/6–47°	0.40 ± 0.04	0.83 ± 0.02

[a]P = P-wave, R1 RSTF = short-arc Rayleigh wave relative source time functions, hrGPS = three-component high-rate (30-second sample interval) GPS, SH = SH wave, surface = long-period surface waves, GPS = static GPS with components listed.
[b]"Variable" listed for curved slab geometries.
[c]Correlation between estimated coseismic slip and interseismic coupling (with no coupling at the trench and coupling permitted at the trench).

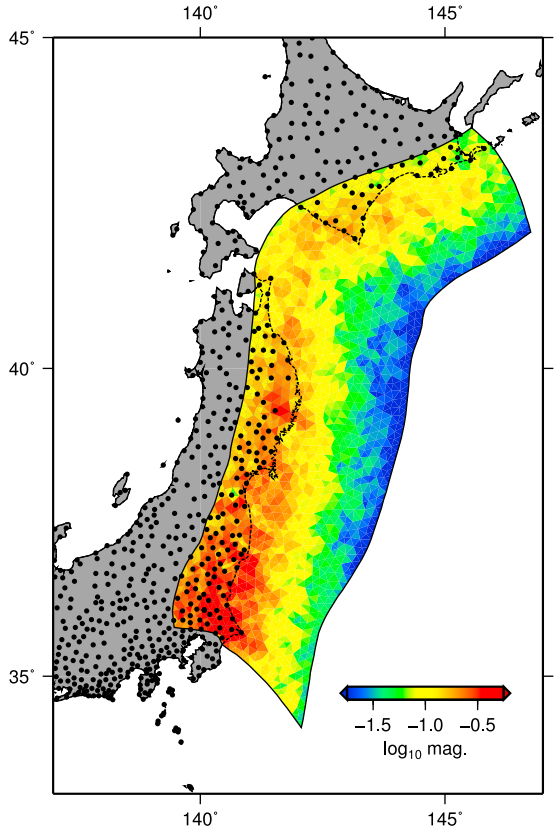

Figure 3. Power of GEONET GPS stations to constrain plate interface behavior. Each element is colored by the sum of the displacements at GPS stations (dots) due to unit strike- and dip-slip on that element (i.e., sum of the partial derivatives relating GPS displacement to unit slip).

(20–60 km) (Figure 3). A simple estimate of the extent to which coseismic slip distributions are spatially coincident with interseismic coupling distributions may be determined by calculating the correlation coefficient between the two spatially variable fields. Coseismic slip distributions resolved from inversions of GPS data show strong correlation (≥0.8) with the pre-seismic coupling distribution [*Loveless and Meade*, 2010] (Figures 2d, 2e, S4, S5, S7; Table 1).[1] Relaxing the assumption of zero interseismic coupling along the Japan trench yields strong (≥80%) coupling shifted trenchward (Figures 1c and 2), while providing a slightly better fit to the interseismic GPS data due to fewer boundary conditions (mean residual GPS speed of 1.71 mm/yr vs. 1.84 mm/yr in the constrained case). Slip distributions inferred from teleseismic data show peak slip close to the subduction trench and are better correlated with this modified coupling distribution (Figures 2b, 2c, 2f, S2, S3, S6; Table 1). Exceptions are the teleseismic inversion of Ammon et al. (in press, 2011), which yields a slip distribution correlated equally with the reference and adjusted coupling distributions (Figure S1; Table 1), and the preferred slip distribution of this study, with slip near the trench permitted, which shows a strong correlation with the modified coupling distribution (Figure S8; Table 1).

[1]Auxiliary materials are available in the HTML. doi:10.1029/2011GL048561.

[8] The above comparisons indicate that the Tohoku-oki earthquake ruptured some portions of the plate interface that experience substantial aseismic slip during the interseismic period. The spatial extent of the concentration of strongest (≥80%) coupling around Sendai (Figure 1a) is far smaller (7.4×10^3 km^2) than both the rupture area of the Tohoku-oki earthquake (8.5×10^4 km^2) and the ≥80% coupled region offshore Hokkaido that encompassed the 2003 $M_W \sim 8.0$ Tokachi-oki earthquake (2.2×10^4 km^2). Past seismicity offshore Sendai was characterized by M ~ 7.0 earthquakes, recently demonstrated by 3 events that occurred 2003–2005. While these smaller events were located within or nearby the most strongly interseismically coupled region (Figure 1a), the Tohoku-oki event indicates that earthquakes can propagate into regions inferred to be less strongly coupled (<80%; as low as 30%), and that more frequent, smaller magnitude earthquake behavior is occasionally punctuated by the occurrence of much larger events that break multiple asperities [*Kaneko et al.*, 2010; *Simons et al.*, 2011].

[9] The saddle of low magnitude (≤20%) coupling between the Sendai and Hokkaido concentrations (Figure 1a) coincides with the location of the 1994 $M_W = 7.6$ Sanriku-oki earthquake and its associated region of postseismic afterslip [*Heki et al.*, 1997]. A postseismic deformation signal following that earthquake is likely to be represented to some extent in the 1996–2000 GPS time series used to estimate interseismic coupling [*Loveless and Meade*, 2010]. Therefore, the northern extent of the off-Sendai concentration of coupling may be defined by deformation related to the 1994 earthquake where ongoing low magnitude (~10 mm/yr) coseismic sense slip at depth may have prevented the continued accumulation of interseismic strain until at least 2000. In other words, had the 1994 Sanriku-oki earthquake not occurred, it is possible that interseismic coupling inferred from GPS data spanning 1996–2000 may have been more spatially homogeneous along the strike of the subduction zone. Detailed studies of GPS time series in this region have been ambiguous with regard to the timescale for the decay of postseismic deformation and a return to nominally interseismic behavior [*Nishimura et al.*, 2004]. Regardless, the northern limit of the rupture areas of $M_W \sim 9$ earthquakes offshore Honshu, such as the Tohoku-oki earthquake, may be defined by a temporal change in stress state caused by previous slip events earthquake, or a longer-lived heterogeneity in subduction interface properties.

3. Discussion

[10] A primary goal of geodetic imaging of earthquake cycle processes is to understand the extent to which coseismic slip distribution is spatially coincident with interseismic coupling distribution. We find general agreement between the spatial extent of coseismic slip from eight different inversions and the region coupled ≥30% before the earthquake (Figures 1 and 2): the estimated rupture length (36–40°N) and latitude of peak slip (38.2°N) are similar to the latitudinal extent and maximum coupling of the reference coupling distribution (Figure 1), but there is substantial variation in the details of estimated coseismic slip, including the longitude/depth of peak slip (Figures 1 and 2). Though slip inversions utilizing spatial regularization (smoothing) have perfect model resolution in terms of a diagonal model resolution matrix, the ability of the data to constrain fault behavior

varies as a function of relative fault-observation geometry. The impact of each triangular dislocation element (TDE) used in our inversions on the estimated slip distribution can be represented by summing the displacements at all GPS stations in response to unit slip on that element (Figure 3). Elements beneath the coastline (40–50 km depth) have the largest partial derivatives (relating GPS displacement to TDE slip) and thus slip on them is best constrained by the available data. The least well-constrained portion of the subduction interface is located near the trench between 36–40°N latitude, roughly coincident with the along-strike extent of the Tohoku-oki earthquake.

[11] While the relative distance of the GPS data in Honshu limits the ability to robustly resolve near-trench behavior, substantial shallow coseismic slip has been inferred from both seismic and geodetic data (Figures 1 and 2). These estimates are consistent with the idea that the shallowest part of a subduction zone is capable of slipping coseismically. The question is whether slip at shallow depths is a result of dynamic overshoot [*Ide et al.*, 2011] or represents the release of elastic strain accumulated in the shallowest crust during the interseismic phase of the seismic cycle. The former idea is consistent with arguments based on rate-and-state friction [e.g., *Liu and Rice*, 2005] and material properties [e.g., *Oleskevich et al.*, 1999] that suggest that the shallow megathrust is characterized by velocity strengthening material, which is likely to creep during the interseismic period. In contrast, the second idea is more consistent with isolated seafloor geodetic observations that suggest interseismic coupling as shallow as 2 km depth on the Nazca-South American subduction interface offshore Peru [*Gagnon et al.*, 2005]. Our previously published reference coupling distribution [*Loveless and Meade*, 2010] assumed no interseismic coupling near the trench, but the alternate solution presented here demonstrates that interseismic GPS velocities are also consistent with strong coupling at the shallowest portion of the interface. In regions where geodetic data are collected closer to the trench than in Honshu, as is the case along the Nankai subduction zone in southwest Japan, and as will be the case when dense networks of seafloor GPS are deployed along worldwide subduction zones, better constraints may be placed on the nature of shallow subduction zone seismic cycle processes, including the correlation of interseismic coupling and coseismic slip in megathrust earthquakes.

[12] **Acknowledgments.** We thank Sue Owen for providing access to the horizontal coseismic GPS displacements used in the slip inversion; Charles Ammon, Andreas Hoechner, and Shinzaburo Ozawa for sharing their coseismic slip distributions via email; and Glen Mattioli and an anonymous referee for helpful reviews. This work was supported by Harvard University.

[13] The Editor thanks Glen Mattioli and an anonymous reviewer for their assistance in evaluating this paper.

References

Aki, K. (1979), Characterization of barriers on an earthquake fault, *J. Geophys. Res.*, *84*, 6140–6148, doi:10.1029/JB084iB11p06140.

Ammon, C., T. Lay, H. Kanamori, and M. Cleveland (2011), A rupture model of the great 2011 Tohoku earthquake, *Earth Planets Space*, doi:10.5047/eps.2011.05.015, in press.

Cloos, M. (1992), Thrust-type subduction-zone earthquakes and seamount asperities: A physical model for seismic rupture, *Geology*, *20*, 601–604, doi:10.1130/0091-7613(1992)020<0601:TTSZEA>2.3.CO;2.

DeMets, C., R. G. Gordon, and D. F. Argus (2010), Geologically current plate motions, *Geophys. J. Int.*, *181*, 1–80, doi:10.1111/j.1365-246X.2009.04491.x.

Furuse, N., and Y. Kono (2003), Slab residual gravity anomaly: Gravity reduction due to subducting plates beneath the Japanese Islands, *J. Geodyn.*, *36*, 497–514, doi:10.1016/S0264-3707(03)00062-0.

Gagnon, K., C. D. Chadwell, and E. Norabuena (2005), Measuring the onset of locking in the Peru–Chile trench with GPS and acoustic measurements, *Nature*, *434*, doi:10.1038/nature03412.

Gander, W., G. H. Golub, and R. Strebel (1994), Least-squares fitting of circles and ellipses, *BIT Numer. Math.*, *34*(4), 558–578, doi:10.1007/BF01934268.

Hashimoto, C., A. Noda, T. Sagiya, and M. Matsu'ura (2009), Interplate seismogenic zones along the Kuril–Japan trench inferred from GPS data inversion, *Nat. Geosci.*, *2*, 141–144, doi:10.1038/ngeo421.

Heki, K., S. Miyazaki, and H. Tsuji (1997), Silent fault slip following an interplate thrust earthquake at the Japan Trench, *Nature*, *386*, 595–598, doi:10.1038/386595a0.

Hoechner, A., A. Y. Babeyko, and S. V. Sobolev (2011), Geodetic source model for the 2011 Tohoku earthquake and tsunami, paper presented at EGU General Assembly, Vienna, Austria.

Ide, S., A. Baltay, and G. C. Beroza (2011), Shallow dynamic overshoot and energetic deep rupture in the 2011 Mw 9.0 Tohoku-Oki earthquake, *Science*, *332*, 1426–1429, doi:10.1126/science.1207020.

Kaneko, Y., J. P. Avouac, and N. Lapusta (2010), Towards inferring earthquake patterns from geodetic observations of interseismic coupling, *Nat. Geosci.*, *3*, 363–369, doi:10.1038/ngeo843.

Kelleher, J., and W. McCann (1976), Buoyant zones, great earthquakes, and unstable boundaries of subduction, *J. Geophys. Res.*, *81*(26), 4885–4896, doi:10.1029/JB081i026p04885.

Konca, A. O., et al. (2008), Partial rupture of a locked patch of the Sumatra megathrust during the 2007 earthquake sequence, *Nature*, *456*, 631–635, doi:10.1038/nature07572.

Liu, Y., and J. R. Rice (2005), Aseismic slip transients emerge spontaneously in three-dimensional rate and state modeling of subduction earthquake sequences, *J. Geophys. Res.*, *110*, B08307, doi:10.1029/2004JB003424.

Loveless, J. P., and B. J. Meade (2010), Geodetic imaging of plate motions, slip rates, and partitioning of deformation in Japan, *J. Geophys. Res.*, *115*, B02410, doi:10.1029/2008JB006248.

Meade, B. J. (2007), Algorithms for the calculation of exact displacements, strains, and stresses for triangular dislocation elements in a uniform elastic half space, *Comput. Geosci.*, *33*, 1064–1075, doi:10.1016/j.cageo.2006.12.003.

Miura, S., Y. Suwa, A. Hasegawa, and T. Nishimura (2004), The 2003 M8.0 Tokachi-Oki earthquake: How much has the great event paid back slip debts?, *Geophys. Res. Lett.*, *31*, L05613, doi:10.1029/2003GL019021.

Moreno, M., M. Rosenau, and O. Oncken (2010), 2010 Maule earthquake slip correlates with pre-seismic locking of Andean subduction zone, *Nature*, *467*, 198–202, doi:10.1038/nature09349.

Nishimura, T., T. Hirasawa, S. Miyazaki, T. Sagiya, T. Tada, S. Miura, and K. Tanaka (2004), Temporal change of interplate coupling in northeastern Japan during 1995–2002 estimated from continuous GPS observations, *Geophys. J. Int.*, *157*(2), 901–916, doi:10.1111/j.1365-246X.2004.02159.x.

Oleskevich, D. A., R. D. Hyndman, and K. Wang (1999), The updip and downdip limits to great subduction earthquakes: Thermal and structural models of Cascadia, south Alaska, SW Japan, and Chile, *J. Geophys. Res.*, *104*(B7), 14,965–14,991, doi:10.1029/1999JB900060.

Ozawa, S., T. Nishimura, H. Suito, T. Kobayashi, M. Tobito, and T. Imakiire (2011), Coseismic and postseismic slip of the 2011 magnitude-9 Tohoku-Oki earthquake, *Nature*, *475*, 373–376, doi:10.1038/nature10227.

Simons, M., et al. (2011), The 2011 magnitude 9.0 Tohoku-Oki earthquake: Mosaicking the megathrust from seconds to centuries, *Science*, *332*, 1421–1425, doi:10.1126/science.1206731.

Suwa, Y., S. Miura, A. Hasegawa, T. Sato, and K. Tachibana (2006), Interplate coupling beneath NE Japan inferred from three-dimensional displacement field, *J. Geophys. Res.*, *111*, B04402, doi:10.1029/2004JB003203.

J. P. Loveless, Department of Geosciences, Smith College, Northampton, MA 01063, USA. (jloveless@smith.edu)

B. J. Meade, Department of Earth and Planetary Sciences, Harvard University, Cambridge, MA 02138, USA.